Eur. Phys. J. A **19**, 169–172 (2004)
DOI 10.1140/epja/i2003-10180-5

THE EUROPEAN PHYSICAL JOURNAL A

Letter

First identification of excited states in the $T_z = 1/2$ nucleus ^{93}Pd

D. Sohler[1,2,a], K. Lagergren[2], J. Blomqvist[2], B. Cederwall[2], A. Johnson[2], B. Hadinia[2], L. Milechina[2], J. Timár[1], G. de Angelis[3], P. Bednarczyk[4,5], D. Curien[4], A. Gadea[3], and J. Nyberg[6]

[1] Institute of Nuclear Research, Pf. 51, H-4001 Debrecen, Hungary
[2] Department of Physics, Royal Institute of Technology, SE-10691 Stockholm, Sweden
[3] Laboratori Nazionali di Legnaro, Padova, Italy
[4] Institute de Recherches Subatomiques, F-67037 Strasbourg, France
[5] H. Niewodniczanski Institute of Nuclear Physics, Krakow, Poland
[6] Department of Radiation Sciences, Uppsala University, Uppsala, Sweden

Received: 28 October 2003 / Revised version: 4 December 2003 /
Published online: 26 January 2004 –
Communicated by J. Äystö

Abstract. The first experimental information about excited states in the $N = Z + 1$ nucleus ^{93}Pd is presented. The experiment was performed using a 205 MeV ^{58}Ni beam from the Vivitron accelerator at IReS, Strasbourg, impinging on a bismuth-backed ^{40}Ca target. Gamma-rays, neutrons and charged particles emitted in the reactions were detected using the Ge detector array Euroball, the Neutron Wall liquid-scintillator array and the Euclides Si charged-particle detector system. The experimental level scheme is compared with the results of new shell model calculations which predict a coupling scheme with aligned neutron-proton pairs to greatly influence the level structure of $N \approx Z$ nuclei at low excitation energies.

PACS. 21.10.Hw Spin, parity, and isobaric spin – 23.20.Lv γ transitions and level energies – 27.60.+j $90 \leq A \leq 149$ – 21.60.Cs Shell model

The neutron-deficient nuclei in the $A \approx 80$–90 mass region with $N, Z < 50$ are expected to exhibit a rich variety of features. These nuclei are close to the proton drip line as well as to the $N = Z$ line, and are situated near the doubly magic nucleus ^{100}Sn, which is predicted to be the heaviest self-conjugate nucleus with bound states. The vicinity of the $N = Z$ line allows new correlations to emerge, when the protons and neutrons occupy nearly identical orbitals. In addition to the seniority coupling scheme found in nuclei further from the $N = Z$ line and in which protons and neutrons separately couple to spin 0 in the ground state, the nuclei with T_z close to zero may exhibit an aligned proton-neutron pairing, *i.e.* the protons and neutrons form deuteron-like pairs. When leaving the $N = Z$ line, the importance of this effect is expected to decrease rapidly. With $N = Z + 1$, ^{93}Pd is predicted to exhibit the qualities of a transitional nucleus on the boundary between these two extremes. In this work we present the first experimental information about excited states in ^{93}Pd. The proposed level scheme is interpreted in relation to new shell model calculations.

The experiment was performed at IReS, Strasbourg in the spring of 2003. Excited states in ^{93}Pd were populated via the reaction ^{40}Ca(^{58}Ni, αn) using a continuous beam with an energy of 205 MeV and with an average intensity of 5 pnA. The isotopically enriched (99.965%) 6.5 mg/cm^2 thick ^{40}Ca targets used in the reactions were backed with a 1 mg thick Bi layer in order to stop the recoiling product nuclei. An additional Bi layer (250 μg/cm^2) was placed on the other side of the ^{40}Ca targets to protect them from oxidization. The targets were kept in vacuum or in an inert Ar atmosphere at all times to further minimize the risk of ^{16}O contamination. However, due to the heating of the target caused by the constant beam bombardment, small amounts of ^{12}C and ^{16}O contaminants present in the "vacuum" of the target chamber and beam lines were deposited on the targets. The target foils were therefore replaced at regular intervals in order to reduce the amount of reactions between the ^{58}Ni beam and these contaminants.

The γ-rays emitted in the reactions were detected using the EUROBALL detector system [1], at the time of the experiment consisting of 15 cluster-type [2] and 26 clover-type [3] composite Ge detectors. Neutrons evaporating from the compound nuclei were detected using

[a] e-mail: sohler@atomki.hu

the Neutron Wall array [4], which comprised 50 organic liquid-scintillator elements, covering the forward 1π section of the solid angle around the target position. Emitted charged particles, in the present experiment mainly protons and α-particles, were detected by the EUCLIDES [5] Si detector array. This array comprised 40 ΔE-E telescopes, of which the forwardmost 5 were subdivided into 4 segments.

The emission of neutrons are rare events for the studied reactions, which have a compound nucleus far out on the neutron-deficient side of the nuclide chart. It was therefore of vital importance to efficiently identify the neutrons on-line, so that events with detected neutrons could be enhanced by the trigger condition. An event trigger requiring coincidences between one or more neutrons detected by the Neutron Wall and one or more Compton-suppressed γ-rays detected in the Ge detectors was employed. In addition, an alternate trigger condition requiring three or more Compton-suppressed γ-rays (in coincidence with either a neutron or a γ-ray detected in the Neutron Wall) was used during part of the experiment.

The on-line discrimination between neutrons and γ-rays detected by the Neutron Wall was achieved using the zero–cross-over (ZCO) time of the corresponding signals. The zero-crossing usually occurs at a later time for neutrons than for γ-rays. However, piled-up γ-rays can give zero-crossing times that are similar to those of the neutrons. In the off-line analysis, the gating criteria applied to the ZCO parameter were therefore complemented by a requirement placed on the time-of-flight (TOF) parameter of the Neutron Wall data. The TOF of a neutron or a γ-ray is measured relative to the common time reference of the event. The Neutron Wall has an excellent time resolution (of the order of 1 ns), and was therefore in the present experiment chosen to provide this time reference. The reference time is then obtained from the detection time of the first neutron or γ-ray in each event that is registered by the Neutron Wall, and will therefore have a different character depending on whether a prompt γ-ray or a neutron was registered first in the Neutron Wall. Different gating criteria were therefore employed for these cases. Furthermore, a neutron that provides the time reference cannot easily be distinguished from a prompt γ-ray pile-up event, since both the TOF and the ZCO parameters are similar for these interactions. Consequently, the resulting neutron-gated γ-ray spectra will contain a significant amount of background from reaction channels with fewer detected neutrons. Singles spectra created using only events in which a prompt γ-ray had been detected in the Neutron Wall, and thus provided the time reference, were employed to identify the γ-rays that were assigned to ^{93}Pd in this work, while the full statistics were retained for the γ-γ coincidence analysis.

The observed α-particles and protons were identified on the basis of the amount of energy deposited in the ΔE and E detectors of the Euclides Si detector array. The probability to detect and correctly identify an emitted proton was 52%, and the corresponding value for the α-particles was 31% in the present experiment. The inclusion of a neutron in the trigger condition prevents the extraction of the detection efficiency of a single emitted neutron from the present data set, but this value is typically around 25% [4].

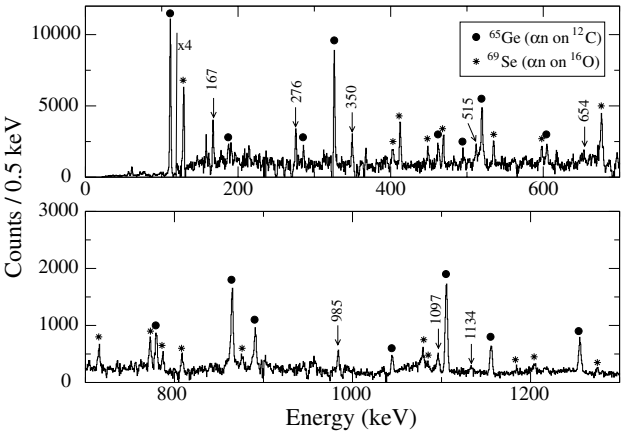

Fig. 1. Background-subtracted spectrum showing the γ-rays assigned to the αn evaporation channel. Transitions indicated by circles and stars are known contaminants from ^{12}C and ^{16}O, respectively. The γ-rays assigned to ^{93}Pd in the present work are indicated by arrows and the corresponding energy values.

Gamma-ray energy spectra and E_γ-E_γ coincidence matrices were created off-line by requiring coincidences with different combinations of detected charged particles and neutrons, and were analyzed using software from the RADWARE package [6]. As a consequence of the limited detection efficiencies, spectra gated by a certain number of particles may contain γ-rays from reaction channels with a higher number of emitted particles. The strongest contributors to this background in the spectrum gated by one α-particle and one neutron, corresponding to ^{93}Pd, were in the present experiment the αpn (^{92}Rh) and α2pn (^{91}Ru) fusion-evaporation channels. In the background-subtracted spectrum (see fig. 1), where the γ-lines of these contaminants have been removed, γ-rays resulting from transitions between high-spin states in ^{65}Ge [7] and ^{69}Se [8] nuclei are visible. These nuclei correspond to the αn channels in reactions between the ^{58}Ni beam and the ^{12}C and ^{16}O target contaminants. These reactions take place closer to stability than the reactions with ^{40}Ca, and can thus contribute a considerable background in the γ-ray spectra, even at relatively low degrees of target contamination. These γ-rays were identified and excluded from the list of possible ^{93}Pd candidates. Also γ-rays arising from possible ^{48}Ca and Mg contaminations in the target were checked and excluded during the analysis.

The energies and intensities of the γ-rays assigned to ^{93}Pd in the present work are given in table 1. Figure 2 shows the intensity ratios for some of these, as measured in coincidence with different numbers of α-particles and neutrons. The same quantities for previously established γ-rays emanating from stronger reaction channels are included in the figure. In the top panel, the intensity ratio for γ-rays detected in coincidence with zero or one α-particle is indicated. The reaction channels corresponding to two

Table 1. The energies, relative intensities and angular-distribution ratios of the γ-rays assigned to ^{93}Pd as deduced from the present work. Statistical uncertainties are given within parentheses.

E_γ (keV)	I_γ (%)	R ratio	E_i (keV)	$I_\mathrm{i}^\pi \rightarrow I_\mathrm{f}^\pi$
166.9(3)	62(6)	0.60(8)	2525	$(21/2^+) \rightarrow (19/2^+)$
275.6(3)	66(7)	0.64(9)	2358	$(19/2^+) \rightarrow (17/2^+)$
349.9(4)	47(8)	0.93(10)	2875	$(25/2^+) \rightarrow (21/2^+)$
350.6(5)	21(6)			
515.1(3)	25(5)	0.59(9)		
654.0(3)	25(3)	1.14(14)	5655	$(37/2^+) \rightarrow (33/2^+)$
984.8(3)	85(6)	0.97(11)	2082	$(17/2^+) \rightarrow (13/2^+)$
992.4(4)	35(5)	0.99(14)	3867	$(29/2^+) \rightarrow (25/2^+)$
1097.4(3)	100(6)	1.15(12)	1097	$(13/2^+) \rightarrow (9/2^+)$
1133.9(4)	27(3)	1.04(15)	5001	$(33/2^+) \rightarrow (29/2^+)$
1635.3(6)	18(2)	1.05(16)	7290	$(41/2^+) \rightarrow (37/2^+)$

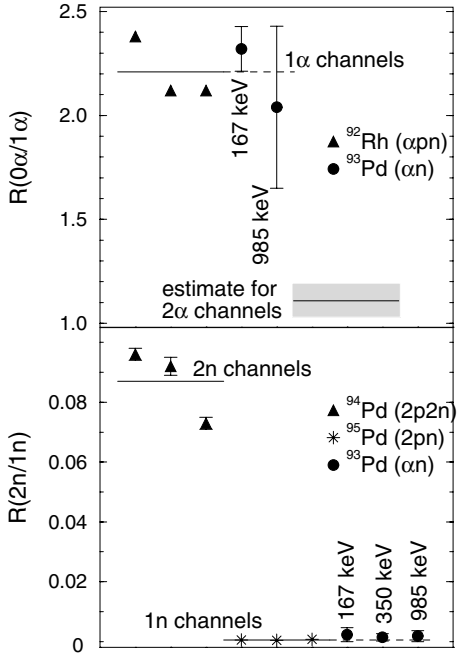

Fig. 2. The top panel shows the intensity ratios of different γ-rays deduced from spectra gated by 0α and 1α. The same ratio for reaction channels corresponding to two emitted α-particles, estimated from the experimentally deduced detection efficiency, is indicated in the figure. The shaded area shows the estimated uncertainty in this ratio. The bottom panel presents similar ratios obtained from spectra gated by 2n and 1n. The same quantities measured for known transitions in ^{92}Rh [9], ^{94}Pd [1,2,4] and ^{95}Pd [3,4] are included for comparison.

emitted α-particles were too weak in the present experiment for the peaks to be visible in spectra gated by a lower number of α-particles. The ratio for these reaction channels was therefore estimated from the experimentally deduced detection efficiency. From fig. 2 it is clear that the 985 keV and 167 keV γ-rays were produced in an αn reaction channel, and that the 350 keV γ-ray belongs to a reaction channel with one emitted neutron. Furthermore, these γ-lines were not seen in coincidence with any detected protons. The statistics and problems with coinciding peaks from other reaction channels did not allow for these ratios to be deduced for the other γ-rays assigned to this nucleus. However, all γ-rays assigned to ^{93}Pd in the present work were observed to be in coincidence with the 985, 167 and 350 keV γ-rays (see below), thus strengthening their assignment to the αn reaction channel.

The multipolarities of the γ-rays assigned to ^{93}Pd in this work (see table 1) were obtained by means of a simplified angular-correlation analysis. The angular-distribution ratio $R_\mathrm{ang} = (I_\gamma(137°) + I_\gamma(156°))/(I_\gamma(77°) + I_\gamma(103°))$ was obtained from the intensities of the γ-rays detected in different directions around the target. Here I_γ are the intensities of the γ-rays as deduced from spectra gated by the γ-rays assigned to this nucleus and observed at any direction. The quantities $I_\gamma(137°)$ and $I_\gamma(156°)$ are the intensities of the γ-rays detected in the cluster detectors placed at these angles, and the $I_\gamma(77°)$ and $I_\gamma(103°)$ values are the detected intensities of the same γ-rays in the clover detectors. To reduce the uncertainty in the measured R_ang values we determined them from spectra gated by different coincident γ-rays. In this geometry, angular-distribution ratios of known stretched quadrupole transitions have an average value of $R = 1.08$. For known stretched dipole transitions the average value is $R = 0.60$. Based on the measured R_ang values, stretched dipole character was assigned to the 167, 276 and 515 keV transitions, while stretched quadrupole nature was assigned to the 350, 654, 985, 992, 1097, 1134 and 1635 keV γ-rays. The results of the angular-distribution analysis are given in table 1, together with the tentative spins and parities of the initial and final states.

The level scheme for ^{93}Pd as deduced from the present work is given in fig. 3. All the γ-rays that have been placed in the level scheme were found to be in mutual coincidence. The ordering of the γ-rays in the level scheme is based on their relative intensities, with the strongest transitions placed at the bottom of the band. The level at 5001 keV remains ambiguous due to the uncertain ordering of the 1134 and 654 keV transitions. The 350 keV γ-ray was found to be a self-coincident doublet, but only one of the 350 keV transitions could be placed in the level scheme due to lack of statistics. Due to this doublet transition, the placement of the 515 keV transition remains somewhat uncertain. There is also a second, very weak but significant, 515 keV doublet. This transition most probably feeds the band at either of the tentative $21/2^+$ and $25/2^+$ states, although the latter assignment seems to be favored by the coincidence data. A sum of background-subtracted γ-ray spectra is shown in fig. 4, gated by the γ-rays that were assigned to ^{93}Pd, detected in coincidence with one neutron and one α-particle.

From β-decay studies [10] and previous shell model calculations [11] the ground state has been predicted to have a spin and parity of $7/2^+$ or $9/2^+$. The new shell model calculations reported in this work favor the $9/2^+$ assignment, and we thus adopt this as our tentative ground

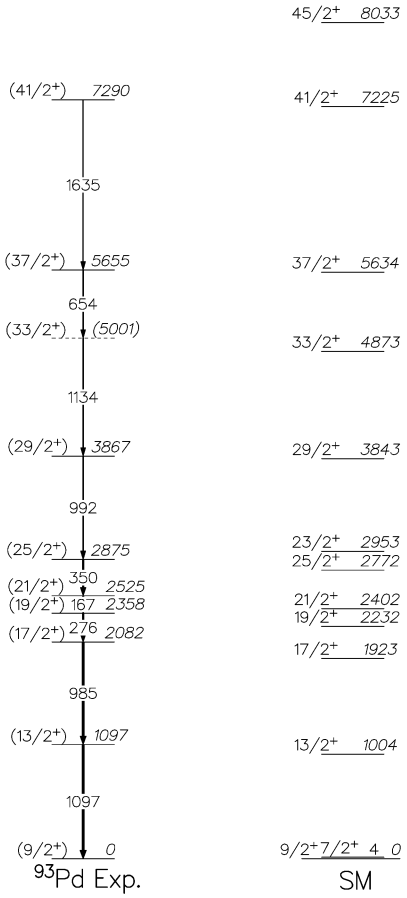

Fig. 3. The proposed level scheme of ^{93}Pd populated in the reaction ^{40}Ca(^{58}Ni, αn). The results of shell model calculations are included in the right part of the figure.

state. The spin assignments of the excited states were based on the assumption that the spins increase as a function of increasing excitation energy, which is reasonable since these levels were populated in a fusion-evaporation reaction experiment. The quadrupole transitions were assumed to be stretched and have electric character, *i.e.* they connect states of equal parity. The stretched dipole transitions were assumed to have magnetic character, based on comparisons with shell model predictions.

The shell model calculation for ^{93}Pd was performed in the restricted model space of $g_{9/2}$, $p_{1/2}$ for proton and neutron holes. The single-particle energies and effective interaction matrix elements were taken from an analysis [12] of level energies in nuclei with $38 \leq Z \leq 44$. The calculation was normalized to energy 0 for the $9/2^+$ ground state. The results of our calculation which can be seen to the right in fig. 3 show a good agreement with the experimental level scheme.

The $g_{9/2}$ shells play a dominant role in forming the structure of the states in $N \approx Z$ nuclei below ^{100}Sn. The proton-neutron 9^+ interaction is so strongly attractive that it tends to break the monopole pairing coupling scheme, in favor of an aligned coupling scheme with

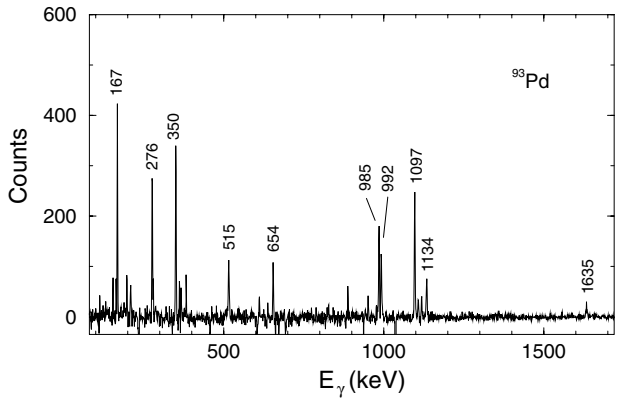

Fig. 4. The sum of background-subtracted spectra gated by the 167, 276, 350, 515, 654, 985 and 1635 keV γ-rays is shown. A coincidence with one detected α-particle and one neutron was also required. The energies of the transitions assigned to ^{93}Pd in the present work are indicated. The energy dispersion is 1 keV/channel.

the angular momenta of protons and neutrons maximally oriented parallel or antiparallel to a fixed axis. This generates a prolate matter distribution, which exerts a (deformation-driving) force on the core particles. Excitations of $g_{9/2}$ particles to the $d_{5/2}$ shell immediately above the shell gaps at $N = 50, Z = 50$ will especially tend to enhance the deformation. However, the good agreement seen in fig. 3 indicates that core excitation effects are still moderate in ^{93}Pd.

This work has been supported by the Swedish Research Council, the European Community - Access to Research Infrastructures action of the Improving Human Potential Programme (contract EUROVIV: HPRI-CT-1999-00078), the Hungarian Fund for Scientific Research (OTKA Contract No. D34587, T038404), the Bolyai János Foundation and the Göran Gustafsson Foundation. The authors thank E. Farnea for his contribution to the experiment.

References

1. J. Simpson, Z. Phys. A **358**, 139 (1997).
2. J. Eberth *et al.*, Nucl. Instrum. Methods A **369**, 135 (1996).
3. G. Duchêne *et al.*, Nucl. Instrum. Methods A **432**, 90 (1999).
4. Ö. Skeppstedt *et al.*, Nucl. Instrum. Methods A **421**, 531 (1999).
5. A. Gadea *et al.*, LNL/INFN (Report) **118/97**, 225 (1997).
6. D. Radford, Nucl. Instrum. Methods A **361**, 297; 306 (1995).
7. D. Sohler *et al.*, Z. Phys. A **357**, 239 (1997).
8. D.G. Jenkins *et al.*, Phys. Rev. C **64**, 064311 (2001).
9. D. Kast *et al.*, Z. Phys. A **356**, 363 (1997).
10. K. Schmidt *et al.*, Eur. Phys. J. A **8**, 303 (2000).
11. H. Herndl, B.A. Brown, Nucl. Phys. A **627**, 35 (1997).
12. R. Gross, A. Frenkel, Nucl. Phys. A **267**, 85 (1976).